

Contact Properties of Tubular Crimp Connections: Elementary Considerations

R.S. Timsit

Timron Advanced Connector Technologies
(Division of Timron Scientific Consulting Inc.),
Toronto, ON, CANADA M5M 1L6
rtimsit@timron-inc.com

Abstract — The paper reviews the fundamental principles of mechanical crimp connections and provides a simple predictive model for achieving acceptable tubular crimps with a solid conductor. This model is based on well-established strain-strain relationships of cylindrical bodies in elasticity mechanics. The model is used to relate the residual contact load in the crimp junction to the mechanical yield strength and elastic springback properties of both the conductor and the crimp barrel. It is shown that the relative yield strength and relative elastic modulus of the materials in contact must meet specific conditions to achieve a crimp junction with acceptable strength and electrical contact resistance. The paper also provides an explanation for the minimum compaction required to achieve a reliable electrical crimp connection in stranded wire connections.

Keywords- Crimp connections, compression connections, electrical contacts.

I. INTRODUCTION

Crimp connector technology is widely used for interconnecting electronic devices and for tapping electrical power in high-power distribution networks. In a crimp connection, a bare conductor is attached to the connector by locating the end of the conductor in the gripping section (i.e. the barrel, sleeve or “folding wings”) of the connector, and squeezing the connector and conductor together using a special crimping tool. Crimping causes extensive plastic deformation of the conductor and connector. In order to generate a reliable crimp connection, this deformation must lead to a sufficiently large residual contact force between the connector terminal and the conductor after the crimping tool is released. This residual contact force is determined by the relative elastic springback of the deformed barrel and conductor on release of the crimping tool [1], as will be explained in greater detail later.

The wide range of applications of crimp connections from electronic devices to large power connections in electrical grid networks is addressed in several publications [2 - 4]. Despite these wide-ranging applications, crimp connector design relies largely on an empirical approach with little resort to engineering formulae or other analytical information as is

often done in the design of separable spring-loaded connectors. In the empirical approach, crimp design is often guided by data derived from computer modeling, such as the distribution of residual mechanical stresses in the formed crimp junction [5 - 9]. Design is also guided by data stemming from field experience by satisfying selected but empirical criteria relating to geometrical crimp design and dimensions. For electronic applications, the integrity of a crimp junction is assessed using various geometrical parameters such as crimp height, crimp width, crimp deformation etc. [10, 11]. Integrity is also evaluated in part by the degree of strand compaction in the crimp joint. Crimp integrity is considered excellent if strand compaction is complete, wherein strands are plastically deformed and squeezed together without significant gaps both between themselves and with the connector sleeve walls [1 - 4]. Such a junction is usually characterized by excellent mechanical pull-strength, low electrical resistance and high stability under a variety of mechanical, electrical and thermal stresses [1,2].

The reason for the largely empirical approach to crimp design stems from the complexity of the deformation process in the conductor and connector terminal [5 - 9] and the challenge of describing deformation in relatively simple analytical terms. The present paper proposes a simple analytical guideline for the design of cylindrical crimp connections, particularly where the strands are fully compacted. This paper reviews the fundamental principles of mechanical crimp connections and provides a simple predictive model for achieving an acceptable crimp connection in a cylindrical barrel terminal with a solid or well-compacted conductor. The model is based on well-established strain-strain relationships of cylindrical bodies in elasticity mechanics. It is shown that the relative yield strength and relative elastic modulus of the materials in contact must meet specific conditions to generate a crimp joint with acceptable strength and electrical contact resistance. The paper also provides an explanation for the minimum compaction required to achieve a reliable electrical crimp connection in stranded wire connections.

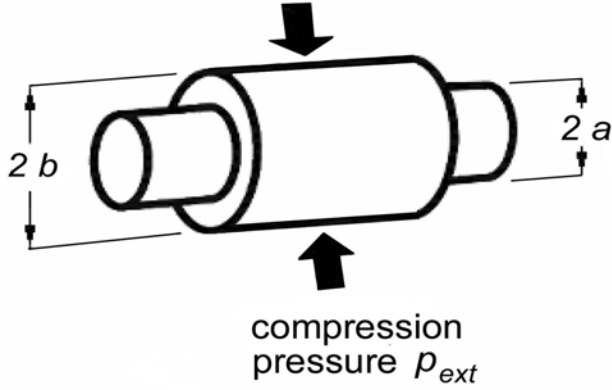


Fig. 1. Schematic diagram of solid conductor in cylindrical barrel.

II. FUNDAMENTAL PRINCIPLES OF A CRIMP CONNECTION

A. Elastic Deformation

We consider the simple situation of a tubular barrel of inner radius a and outer radius b being crimped over a solid cylindrical conductor also of radius a as illustrated schematically in Fig. 1. We will further assume that the materials of both the conductor and barrel are elastic-perfectly plastic as illustrated schematically in Fig. 2. The materials are characterized by an elastic modulus and yield strength respectively of E_B and Y_B for the barrel, and E_C and Y_C for the conductor. Although we consider the case of $Y_C > Y_B$ in the illustrative example considered below, the results will not depend on this assumption. We now follow the sequence of events during crimping.

We assume that the conductor fits into the barrel initially with negligible interference. If a constant and uniform cylindrical pressure p_{ext} is applied over the outer barrel surface, it is known that during elastic deformation (i.e. before plastic flow) the radial and circumferential elastic stress components in the barrel, denoted respectively as $\sigma_{B,r}(r)$ and $\sigma_{B,\theta}(r)$, are given as [10]

$$\sigma_{B,r}(r) = [a^2 b^2 (p_{ext} - p_i) / r^2 + p_i a^2 - p_{ext} b^2] / (b^2 - a^2) \quad (1)$$

and

$$\sigma_{B,\theta}(r) = [-a^2 b^2 (p_{ext} - p_i) / r^2 + p_i a^2 - p_{ext} b^2] / (b^2 - a^2) \quad (2)$$

where $r (\geq a)$ is the radial distance from the center and p_i is the internal pressure generated by the conductor at $r = a$. The radial displacement $u_B(r)$ at radial distance r within the barrel is given as [10]

$$u_B(r) = r [\sigma_{B,\theta}(r) - \nu_B \sigma_{B,r}(r)] / E_B \quad (3)$$

where ν_B is Poisson's ratio for the barrel material. Similarly, the relationships corresponding to Eqs. (1) – (3) for the conductor with $r \leq a$ are [10]

$$\sigma_{C,r}(r) = -p_i \quad (4)$$

$$\sigma_{C,\theta}(r) = -p_i \quad (5)$$

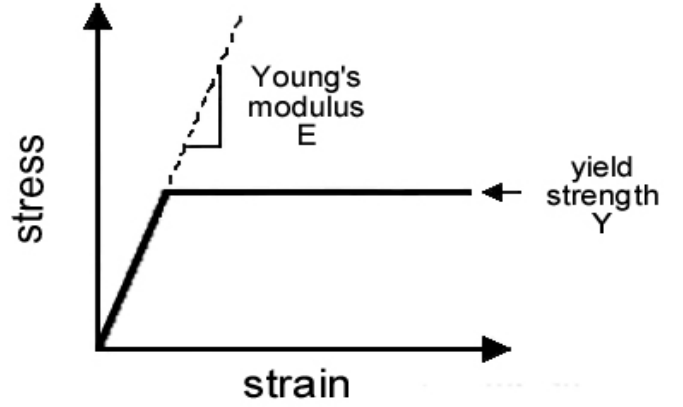


Fig. 2. Stress-strain diagram for an elastic-perfectly plastic material.

with a radial displacement

$$u_C(r) = -r p_i [1 - \nu_C] / E_C \quad (6)$$

where ν_C is Poisson's ratio for the conductor material.

Since the displacements of the conductor and barrel are the same at the boundary $r = a$, the boundary condition $u_B(a) = u_C(a)$ immediately yields the following expression for the pressure p_i in terms of p_{ext}

$$p_i = K^{-1} p_{ext} \quad (7)$$

with

$$K = [(b^2 + a^2) + (1 - \nu)(E_B/E_C)(b^2 - a^2)] / [(b^2 + a^2) + (1 - \nu)(b^2 - a^2)] \quad (8)$$

where we have assumed $\nu_B = \nu_C = \nu$. The pressure p_i at the conductor-barrel interface may be shown to be expressed in terms of the displacement $u_C(a)$ as

$$p_i = \{ K E_C / [a(1 - \nu)] \} u_C(a) \quad (9)$$

where we recall that $u_C(a)$ is the elastic displacement of the conductor surface (and the barrel inner surface) at the location $r = a$. Equation (9) states that the radial stress at the crimping interface increases linearly with displacement, as is expected since the materials behave linearly in the elastic region.

B. Plastic Deformation

We now follow the sequence of events as the applied external stress p_{ext} is increased first to the yield strength of the barrel material and then to the yield point of the conductor material (since $Y_C > Y_B$) during crimping. As illustrated schematically in Fig. 3, the mechanical stress p_i increases linearly along the line OA as the elastic displacement at the conductor-barrel interface is increased, as indicated by Eq. (9). At point A, the crimping stress reaches the yield strength Y_B of the barrel, thus leading to a decrease in the constant K since $E_B \approx 0$ in Eq. (8) beyond the yield point of the barrel. At point

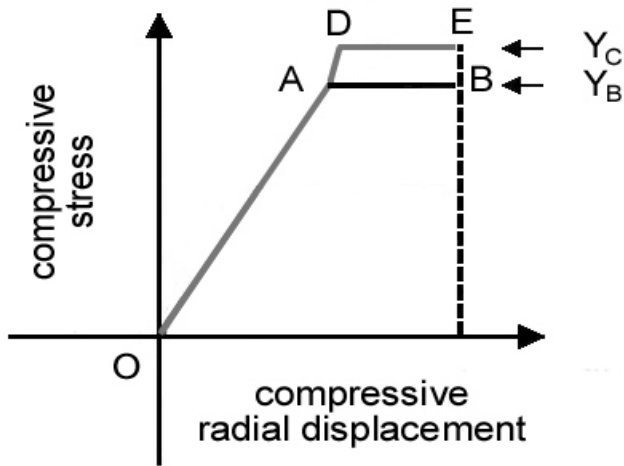
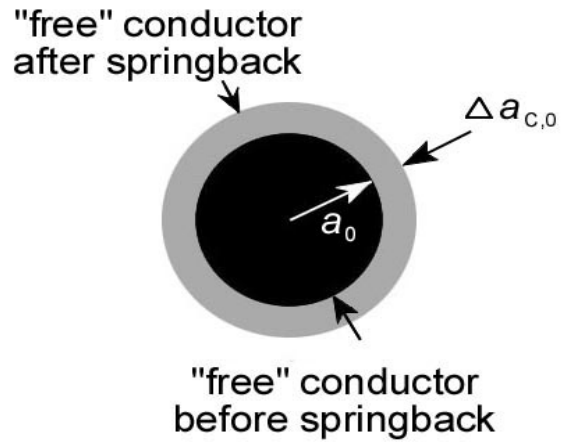


Fig. 3. Variation of the compressive stress p_i at the conductor surface with compressive radial displacement of the conductor.

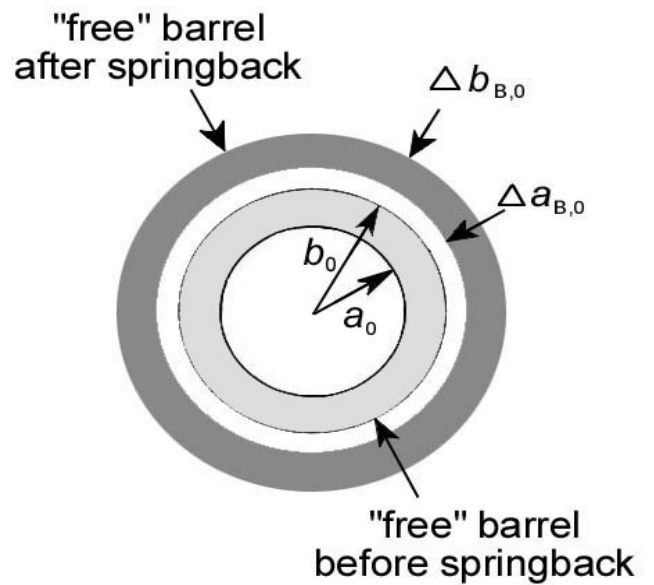
D, the crimping stress reaches the yield strength Y_C of the conductor material and both the conductor and barrel undergo metal flow. Depending on the flow rate and physical constraints of both the barrel and the conductor, the applied stress p_{ext} may increase beyond the yield point of the mating components but the following description does not depend on the maximum value of p_{ext} during crimping. The only quantities of importance are the final radii of the conductor and barrel when crimping is completed and the crimp tool is released. We will assume that the final radius of the conductor (and barrel bore) before release of the crimping tool, is a_0 . The corresponding outer radius of the barrel is denoted as b_0 . These radii are illustrated in Fig. 4(a) and 4(b) respectively. We now consider the events as p_{ext} is suddenly decreased to zero i.e. the crimp tool is released.

C. Formation of Crimp Connection

A heuristic way of understanding the effect of elastic springback is to visualize both the conductor and the barrel as separate “free” isolated objects while still in the state of maximum deformation generated by the crimping tool. At the point of maximum deformation, the radius a_0 of the “free” conductor will be identical with the barrel bore radius. On release of the crimping tool, the visualized “free” isolated objects will spring back elastically to radial dimensions associated with the absence of any applied external load. Such springback will increase both the radius of the “free” conductor by an amount $\Delta a_{C,0}$ and the radius of the “free” barrel bore by an amount $\Delta a_{B,0}$ as illustrated respectively in Figs. 4(a) and 4(b). The outer radius of the barrel will increase by $\Delta b_{B,0}$. If the conductor and barrel are now visualized as reunited, it is clear that an acceptable crimp connection is achieved only if $\Delta a_{C,0}$ exceeds $\Delta a_{B,0}$. In the connection, the final radial extension of the conductor in the barrel will be smaller than $\Delta a_{C,0}$ since the conductor is constrained by the barrel. By the same token, the radial extension of the barrel



(a)



(b)

Fig. 4. Visualization of (a) conductor and (b) barrel as “free” elements before and after elastic springback. The magnitudes of the increase in radius $\Delta a_{C,0}$, $\Delta a_{B,0}$ and $\Delta b_{B,0}$ are exaggerated for ease of illustration.

bore will be larger than $\Delta a_{B,0}$ since the condition $\Delta a_{B,0} < \Delta a_{C,0}$ exposes the barrel to an internal pressure generated by the conductor. Thus the conductor will be in a state of compressive stress while the barrel will be under tensile stress.

We now evaluate the final residual crimping force between the conductor and barrel by referring to the schematic circumferential stress-displacement curves of the separate “free” components, illustrated in Fig. 5, as follows: as soon as the crimping stress on the conductor falls below the yield strength Y_C the conductor returns to elastic deformation and springs back along the line EF (the abscissa in Fig. 5 refers to compressive displacement so a decrease in this displacement along EF corresponds to a springback Δa_C of the conductor).

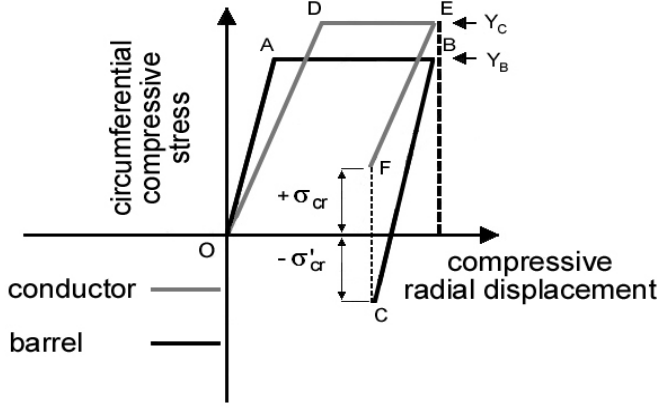


Fig. 5 Generation of circumferential compressive stress at the conductor-barrel interface for the case where $Y_C > Y_B$.

If the crimping stress on the conductor at point F is σ_{cr} then the radial displacement Δa_C of the conductor from the radius a_0 associated with the decrease $(Y_C - \sigma_{cr})$ in compressive stress can be calculated from Eq. (6) as

$$\Delta a_C = u_C(a_0) = a_0 (Y_C - \sigma_{cr}) [1 - \nu] / E_C \quad (10)$$

Similarly, as soon as the crimping stress on the barrel falls below the yield strength Y_B the barrel returns to elastic deformation and springs back along the line BC. If now we re-unite the conductor and barrel so that one fits in the other, two conditions must be satisfied:

- (i) the radial displacement of the conductor Δa_C given by Eq. (10) must match the radial displacement Δa_B of the bore of the barrel and
- (ii) the magnitude of the radial mechanical stress at the conductor surface and at the bore surface of the barrel must be identical.

A crimp is generated where the barrel inner surface is under a radial compressive stress σ_{cr} . The circumferential tensile stress in the barrel at the interface is denoted as $-\sigma_{cr}'$. Points F and C respectively on curves EF and BC in Fig. 5 identify the radial displacement at which these two conditions are satisfied. It is important to note the following features in Fig. 5: the origin "O" associated with the beginning of the deformation process does not apply after plastic deformation. The origin associated with the plastically deformed conductor is located at the point where the extension of line EF crosses the abscissa. The origin associated with the plastically deformed barrel is located at the intersection of line BC with the abscissa. We now evaluate the radial displacement Δa_B of the barrel bore and the final crimping stress σ_{cr} .

From Eqs.(1) and (2), the change in radial and circumferential stresses at the barrel bore surface when the external stress is reduced from Y_B to zero (i.e. when the crimp tool is released) and the internal stress is correspondingly reduced from Y_B to σ_{cr} are given respectively as

$$\Delta \sigma_{B,r}(a_0) = -(\sigma_{cr} - Y_B) \quad (11)$$

$$\text{and} \quad \Delta \sigma_{B,\theta}(a_0) = Y_B + \sigma_{cr}(b_0^2 + a_0^2)/(b_0^2 - a_0^2) \quad (12)$$

From Eqs. (3), (11) and (12), the radial displacement Δa_B of the barrel bore is calculated as

$$\Delta a_B = (a_0 / E_B) \{ (1 - \nu) Y_B + \sigma_{cr} [\nu + (b_0^2 + a_0^2)/(b_0^2 - a_0^2)] \} \quad (13)$$

Using Eq. (13) and the expression for Δa_C from Eq. (10), the crimp condition $\Delta a_B = \Delta a_C$ immediately yields the value of σ_{cr} as

$$\sigma_{cr} = Y_B (r_Y - r_E) / (1 + m r_E / (1 - \nu)) \quad (14)$$

where

$$r_Y = Y_C / Y_B$$

$$r_E = E_C / E_B$$

$$m = \nu + (b_0^2 + a_0^2)/(b_0^2 - a_0^2)$$

On the basis of the present model, Eq.(14) leads to two major conclusions: (i) a crimp connection is generated only where the mating materials are such that $r_Y > r_E$ (or the ratio $S_{YE} = r_Y / r_E > 1$), and (ii) for mating materials satisfying $S_{YE} > 1$ the crimp compressive stress increases linearly with the yield strength Y_C of the conductor. It is important to note that a crimp connection may still be formed where $E_C < E_B$ and $Y_C < Y_B$ provided the condition $S_{YE} > 1$ still holds. The curves illustrating schematically the elastic springback of the conductor and barrel in the latter situation are illustrated in Fig. 6. It may be noted that the crimping stress σ_{cr} in this case is smaller than illustrated in Fig. 5.

III. EXAMPLES OF CRIMP CONNECTIONS

We now evaluate the compressive stress from Eq. (14) for a variety of situations. Table 1 lists typical values of the elastic modulus and yield strength for several materials used in electrical connections. According to the data of Table 1, a cylindrical conductor made of hard-drawn copper cannot be crimped to a tube of cold-worked C26000 brass since this case corresponds to $r_Y = 0.83$ and $r_E = 1.19$ and the condition $S_{YE} > 1$ is not satisfied. On the other hand, the copper conductor can

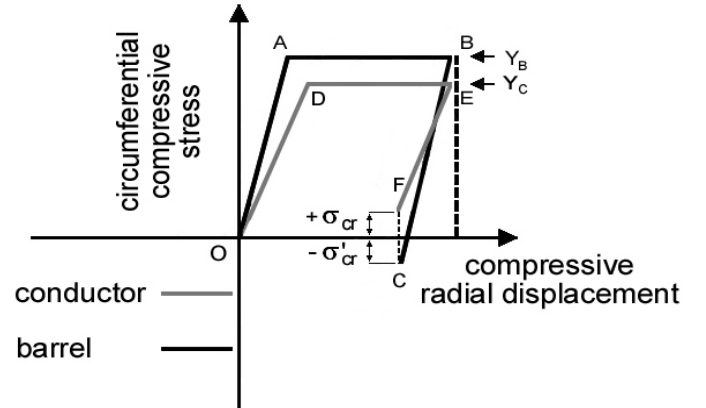


Fig. 6 Generation of circumferential compressive stress at the conductor-barrel interface for the case where $Y_C < Y_B$.

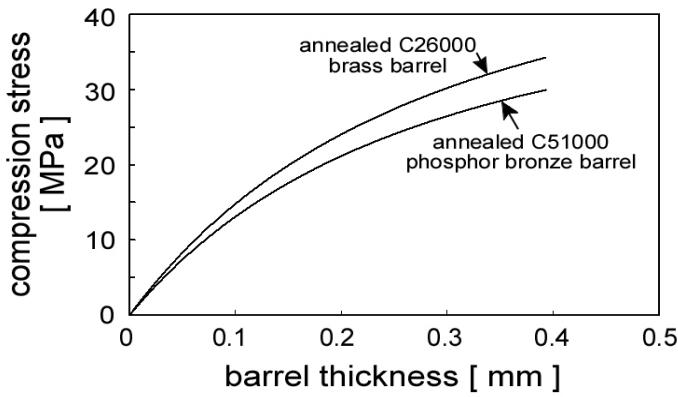


Fig. 7 Compression stress in a crimp connection consisting of solid copper conductor and a cylindrical barrel made from a copper-base alloy.

be crimped to an annealed C26000 tube since in this case r_Y increases to 2.41, thus leading to $S_{YE} > 1$. Similarly, the copper conductor can be crimped to an annealed C51000 tube but not to the same alloy in the hard-drawn condition.

Figure 7 illustrates curves calculated from Eq. (14) showing the compressive stress on a copper conductor as a function of barrel thickness, after the conductor and the barrel have been plastically deformed. The final crimped conductor radius is assumed to be reduced to $a_0 = 0.512$ mm (gauge # 18 wire). The barrel is made from annealed C26000 brass or annealed C51000 phosphor-bronze. The values of Y_C and Y_B used in the calculations are those listed in Table 1 and the Poisson ratio ν is taken as 0.3. The final outer radius of the barrel in Eq. (14) was evaluated as $b_0 = a_0 + d$ where d is the barrel thickness. The data of Fig. 7 indicate that there is not a great deal of difference between the final compression pressure achieved between the copper conductor and either the brass or the phosphor-bronze barrel. In contrast, the conductor cannot be crimped to a tube made from beryllium-copper C17200 in either of the metallurgical conditions shown in Table 1 since the condition $S_{YE} > 1$ is not satisfied in these cases.

Recently, M. Runde and co-workers have reported results of performance tests on a variety of large tubular aluminum compression splices connected to stranded aluminum power conductors [4,11]. Splice performance was assessed on the basis of resistance measurements during short-circuit tests and thermal cycling as specified by the IEC 61238-1 [12] standard, and from inspections of cross-sectioned connections. **It was found** that a large mechanical deformation in a compression splice improved connector performance significantly and that relatively soft (annealed) conductors led to inferior performance than hard-drawn conductors. Soft conductors that hardened significantly during deformation when the splice was installed were also found to pass the tests. All these results are consistent with the predictions of Eq. (14) for the following reason. In the case of an aluminum barrel and a

Table 1: Selected Mechanical Properties of Typical Electrical Contact Materials

Materials	Elastic Modulus [GPa]	Yield Strength [MPa]
copper (oxygen-free, cold-drawn)	119	320
C26000 brass (cold-worked)	100	386
C26000 brass (annealed)	100	133
C51000 phosphor-bronze (hard)	110	581
C51000 phosphor-bronze (annealed)	110	175
C17200 beryllium-copper hardened TF00	127	1,050
C17200 beryllium-copper mill-hardened TM00	127	593
aluminum hard conductor	70	150
aluminum soft conductor	70	82
aluminum barrel	70	78

well-compacted aluminum conductor, the condition $r_E \approx 1$ holds. Since in the work described in [4,11], the barrel was soft to allow for a large deformation during compression we would expect the yield strength Y_B to be relatively small. According to Eq.(14), an acceptable crimp was possible only where $S_{YE} \approx r_Y > 1$ i.e. only where the conductor was significantly harder than the splice material, or was hardened due to deformation during splice installation. This conclusion is further supported by the data of Fig.8.

Figure 8 shows curves calculated from Eq.(14) for a tubular aluminum splice crimped to a solid aluminum conductor. The curves attempt to simulate the experimental conditions

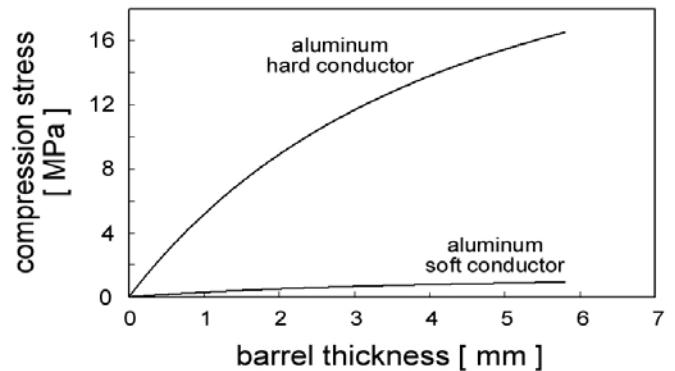


Fig. 8 Compression stress in a crimp connection consisting of solid aluminum conductor and a cylindrical barrel made from an aluminum-base alloy.

described in references [4] and [11] where the initial conductor diameter was 18.2 mm [4]. The curves in the graph describe the compressive stress developed respectively with a soft and a hard conductor as a function of barrel thickness. In these evaluations, the aluminum conductor is assumed to have been plastically deformed to a final conductor diameter of 16.4 mm i.e. $a_0 = 8.2$ mm, from an initial diameter of 18.2 mm. The Vickers hardness of the aluminum barrel was taken as 24 kg mm⁻² [4]. The Vickers hardness of the conductor was assumed as 46 kg mm⁻² and 25 kg mm⁻² respectively for the hard and for the soft aluminum conductor [4]. If the Vickers harness is denoted as H, the value of the yield strength is given as $H / 3$ to a good approximation [13]. The values of Y_C and Y_B used in the evaluations of compression stress, and calculated from the Vickers harness, are listed as the last two entries in Table 1. The Poisson ratio ν is taken as 0.3.

The data of Fig. 8 indicate that the compression pressure achieved with the hard alloy is considerably larger than the pressure generated with the soft alloy. This result also indicates that the electrical contact resistance generated in the compression joint should be smaller with the hard alloy than with the soft alloy, in the absence of a significant difference in the electrical resistivity of the two alloys. On the basis of the results shown in Fig. 8, we conclude that the electrical joint achieved with the hard alloy should be the more reliable. This conclusion is indeed consistent with the experimental findings of Runde et al [4,11].

V. CONNECTIONS WITH STRANDED CONDUCTOR

The formation of a crimp connection between a cylindrical barrel and a stranded conductor is similar to that generated with a solid conductor, but only after the strands have been fully compacted and if the mechanical stress across the entire conductor cross section varies uniformly. The degree of barrel deformation required to achieve full compaction may be estimated as follows.

Detailed evaluations of the packing density of identical cylindrical strands within one large cylinder as illustrated in Fig. 9(a) [14,15] show that the minimum void density reaches about 20%, but only for a sufficiently large number of undeformed strands. Results of these detailed evaluations, showing the dependence of the “minimum” void fraction on the number N of undeformed strands of radius r packed into a cylinder of radius R , are indicated in Fig. 9(b). In this graph, note that the jagged shape of the curve is real and stems from changes in the geometrical arrangement of the packed cylinders as more small cylinders are packed into the holding tube. The above-listed evaluations thus suggest that, for a sufficiently large number of cylindrical strands, the cross-sectional area of a crimp barrel would have to be reduced by about 20% to achieve full strand compaction. It is only after such compaction that the Eq. (14) would be applicable to a cylindrical stranded crimp connection.

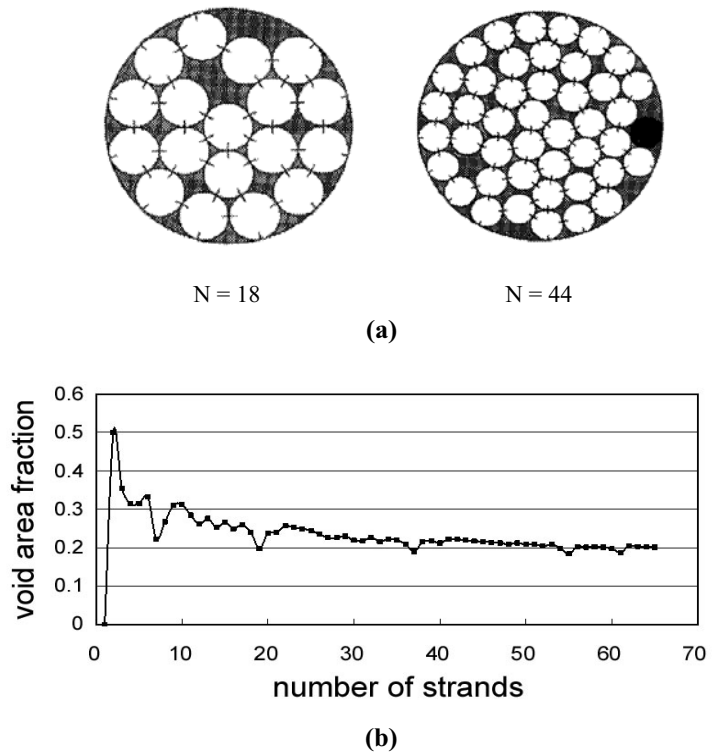


Fig. 9 (a) Examples of packing of circles in a larger circle [15], (b) void density as a function of number of circles calculated from reference [15].

V. SUMMARY

The paper has reviewed fundamental principles underlying the formation of mechanical crimp connections and provides a simple predictive model for achieving acceptable tubular crimps with a solid conductor. This model is based on well-established stress-strain relationships of cylindrical bodies in elasticity mechanics to relate the residual contact load in the crimp junction to the mechanical yield strength and elastic springback properties of both the conductor and the crimp barrel. On the basis of this model, it has been shown that the relative yield strength and relative elastic modulus of the materials in contact must meet specific conditions to achieve a crimp junction with acceptable contact stress and hence acceptable electrical contact resistance.

REFERENCES

- [1] R.W. Rollings, “Design of Reliable Separable Power Connector with Base Metal Contacts for Telephone Equipment Applications”, IEEE Trans. Parts, Hybrids, Packaging, PHP-11, p. 45, 1975.
- [2] R. S. Mroczkowski, **Electrical Connector Handbook**, McGraw-Hill, New York, 1998.
- [3] T.M. Shoemaker and J.E. Mack, **The Lineman’s and Cableman’s Handbook**, chapter 23, McGraw-Hill, New York, 2007.

- [4] M. Runde, H. Jensvold, H. and M. Jochim, "Compression Connectors for Stranded Aluminum Power Connectors", IEEE Trans. Power Delivery, 19, p. 933, 2004.
- [5] S. Kugener, "Simulation of the Crimping Process by Implicit and Explicit Finite Element Methods", AMP J. Technology, 4, p. 8, 1995.
- [6] T. Morita, K. Ohuchi, M. Kaji, Y. Saitoh, J. Shioya, K. Sawada, M. Takahashi, T. Kato and K. Murakami, "Numerical Model of Crimping by Finite Element Method", Proc. 41st IEEE Holm Conf. on Elect. Contacts, p. 151, 1996.
- [7] G. Villeneuve, D. Kulkarni, P. Bastnagel and D. Berry, "Dynamic Finite Element Analysis Simulation of the Terminal crimping Process", Proc. 41st IEEE Holm Conf. on Elect. Contacts, p. 156, 1996.
- [8] G. Rosazza Prin, T. Courtin and L. Boyer, "A New Method to Investigate Electrical Conduction in Crimp Joints: Influence of the Compaction Ratio and Electrical Model", Proc. 48th IEEE Holm Conf. on Elect. Contacts, p. 246, 2002.
- [9] S. Ogihara, K. Takata, Y. Hattori and K. Yoshida, "Mechanical Analysis of the Crimping Connection", Proc. 52nd IEEE Holm Conf. on Elect. Contacts, p. 89, 2006.
- [10] S.P. Timoshenko and J.N. Goodier, **Theory of Elasticity**, McGraw-Hill, New York, 1987.
- [11] M. Runde, R.S. Timsit and N. Magnusson, "Laboratory Performance Tests on Aluminum Splices for Power Conductors", Proc. 24th Int. Conf. Electrical Contacts, p. 157, 2008.
- [12] Compression and Mechanical Connectors for Power Cables with Copper or Aluminium Conductors, IEC Int. Standard 61238-1, 2nd ed., 2003.
- [13] D. Tabor, **The Hardness of Metals**, Oxford, Clarendon Press, 1951.
- [14] S. Kravitz, "Packing Cylinders into Cylindrical Containers", Math. Mag., 40, p. 65, 1967.
- [15] R.L. Graham, B.D. Lubachevsky, K.J. Nurmela and P.R.J. Ostergard, "Dense Packing of Congruent Circles in a Circle", Discrete Math., 181, p. 139, 1998.

Dr. Roland S. Timsit spent 20 years in R&D in the aluminum industry where he carried out extensive work on the properties of copper and aluminum electrical connections, lubrication, brazing and other surface technologies. In 1994, he joined AMP Inc. as Director of Research and was later appointed Director of Technology and Chief Technologist. He is recipient of the IEEE Ragnar Holm Achievement Award and four additional international awards relating to electrical contacts and metal joining. Dr. Timsit is author of over 120 papers and 15 patents. He is currently President of Timron Scientific Consulting Inc., Toronto, Canada, a company serving the technology needs of electrical and electronic connector manufacturers and users.